PERGAMON

International Journal of Solids and Structures 39 (2002) 5481–5494

INTERNATIONAL JOURNAL OF SOLIDS and STRUCTURES

www.elsevier.com/locate/ijsolstr

# Elastic waves from localized sources in composite laminates

Ajit Mal *

*School of Engineering and Applied Science, Mechanical and Aerospace Engineering Department, University of California, Los Angeles, CA 90095-1597, USA*

Received 1 October 2001; received in revised form 18 February 2002

**Abstract**

This paper is concerned with the analysis of elastic waves generated by localized dynamic sources in structural composites. The source can be external, involving acoustic wave loading as in the so called leaky Lamb wave experiment, and low-velocity foreign object impact on the surface of the structure, or internal, as in sudden crack initiation and its rapid growth from existing internal flaws. All three problems are of critical importance in the safe operation of composite structures, due to their vulnerability to hidden delaminations that can occur in composite materials when they are subjected to this type of loads. It is well known that both the dynamic surface loading associated with impact, and the sudden "opening" of an internal crack associated with the extension of a preexisting flaw act as sources of elastic waves in the material of the structure. The research reported here consists of model-based analysis of the guided waves generated by surface loading and microcrack initiation in graphite epoxy composite laminates commonly used in aircraft and aerospace structures. The objective of this study is to develop a mechanics based understanding of the causal relationship between the properties of the source and the characteristics of the waves generated by its initiation and propagation. The results of this research are expected to be useful in developing effective health monitoring systems for new as well as aging aircraft and aerospace structures.


*Keywords:* Composite laminates; Matrix cracking; Fiber break; Delamination; Acoustic emission; Guided waves

## 1. Introduction

Fiber-reinforced composites are being used increasingly as primary structural components in aircraft and aerospace structures as well as in ground and marine transportation. These materials have highly desirable engineering properties, notably, relatively low weight accompanied by high strength and damage tolerance that can be exploited to design structures with high demands on their performance. They also offer a unique mix of formability and other processing advantages over conventional metals. However, composites are very sensitive to the presence of manufacturing flaws and service conditions that can lead to a serious degradation in their load carrying capacity. Another major concern is the growth of undetected hidden delaminations caused by low velocity foreign object impact. Both types of damage, if undetected,

* Tel.: +1-310-825-5481; fax: +1-310-206-4830.
*E-mail address:* ajit@ucla.edu (A. Mal).

0020-7683/02/$ - see front matter © 2002 Elsevier Science Ltd. All rights reserved.
PII: S0020-7683(02)00360-8

can grow to a critical size and lead to catastrophic failure of the structure. In order to insure the safety of the structure, it is often necessary to carry out expensive and extremely time-consuming inspection procedures at regular intervals. The availability of a practical, on board, damage monitoring system in aircraft and aerospace structures can be extremely helpful in improving their safety and reducing maintenance cost by a significant amount.

The sudden occurrence of small flaws initiated from damage sites in structural solids generates elastic waves that carry important information on the nature of the damage. Careful analysis of the waves can reveal the characteristics of the fracture process and the damage. A coordinated theoretical and experimental program of research is being carried out by the author and his associates in an effort to develop the knowledge base required for the design of a practical damage monitoring system in composite structures consisting of distributed surface mounted or embedded multiple sensors. One of the issues that has been studied carefully under this project is the relationship between the properties of the source and the characteristics of the guided elastic waves in composite laminates. The major findings of these studies are summarized in this paper.

An extensive review of published research on low velocity as well as ballistic impact on laminated composites has been given by Abrate (1998). The focus of this research is wave propagation effects associated with impact. Research in this area has been very limited to date. Mal and Lih (1992), and Lih and Mal (1992, 1995, 1996) investigated the response of unidirectional as well as multidirectional composite laminates of infinite lateral dimensions to localized dynamic loads through theoretical modeling and laboratory tests. In contrast to the impact problem, studies on the waves generated by internal sources in structural composites, is rather sparse. Guo et al. (1996) carried out laboratory experiments and theoretical modeling to study the characteristic of the guided waves generated by crack initiation in thin composite laminates.

In this paper an overview of the theoretical and experimental studies carried out by the author's group to characterize the properties of the elastic waves generated by both types of sources, namely, localized surface loads and the initiation of embedded microcracks, is presented. The potential applications of this research in developing effective health monitoring systems for aerospace and aircraft structures are discussed.

## 2. Theory of wave propagation in composites

The behavior of elastic waves propagating through a composite material is determined by its elastic properties. Since composites are highly heterogeneous and anisotropic materials, a number of assumptions need to be made in creating their models that can be treated under the framework of elastodynamic theories. For fiber reinforced graphite/epoxy materials, the homogeneous, and transversely isotropic medium with symmetry axis along the fibers has been found to be quite reasonable in capturing the behavior of the waves in the frequency range of interest in low velocity impact and microcrack extension. This is due to the fact that the diameter of the graphite fibers (5–10 μm) is significantly smaller than the wavelength (of about 100 μm) at frequencies up to 20 MHz, which is well above the frequency range of interest in the problems of interest here. Assuming that the symmetry is along the $x_1$-axis the constitutive relation for the material can be expressed in the frequency domain in the form (see, e.g., Mal and Singh, 1991).

$$\begin{Bmatrix} \bar{\sigma}_{11} \\ \bar{\sigma}_{22} \\ \bar{\sigma}_{33} \\ \bar{\sigma}_{23} \\ \bar{\sigma}_{31} \\ \bar{\sigma}_{12} \end{Bmatrix} = \begin{bmatrix} C_{11} & C_{12} & C_{12} & 0 & 0 & 0 \\ C_{12} & C_{22} & C_{23} & 0 & 0 & 0 \\ C_{12} & C_{23} & C_{22} & 0 & 0 & 0 \\ 0 & 0 & 0 & C_{44} & 0 & 0 \\ 0 & 0 & 0 & 0 & C_{55} & 0 \\ 0 & 0 & 0 & 0 & 0 & C_{55} \end{bmatrix} \begin{Bmatrix} \bar{u}_{1,1} \\ \bar{u}_{2,2} \\ \bar{u}_{3,3} \\ \bar{u}_{2,3} + \bar{u}_{3,2} \\ \bar{u}_{1,3} + \bar{u}_{3,1} \\ \bar{u}_{1,2} + \bar{u}_{2,1} \end{Bmatrix} \tag{1}$$

where $\bar{\sigma}_{ij}$ is the (Fourier time) transform of the Cauchy's stress tensor, $\bar{u}_i$ is the transform of displacement components, $C_{44} = (C_{22} - C_{23})/2$ and the five independent stiffness constants of the material are $C_{11}$, $C_{12}$, $C_{22}$, $C_{23}$ and $C_{55}$.

Modeling the effective elastic moduli of composite materials has been the topic of many studies. For low frequencies and low fiber concentration, the theoretical prediction of the effective elastic constants is in good agreement with experimental results. On the other hand, for high frequencies the theoretical estimates are not satisfactory since the effect of wave scattering by the fibers becomes significant. For fiber-reinforced composite materials, dissipation of the waves is caused by the viscoelastic nature of the resin and by multiple scattering from the fibers as well as other inhomogeneities. Both of these effects can be modeled by assuming complex and frequency-dependent stiffness constants, $C_{ij}$, in the form (Mal et al., 1992a),

$$C_{11} = \frac{c_{11}}{1 + \mathrm{i}p\sqrt{c_{55}/c_{11}}}, \quad C_{22} = \frac{c_{22}}{1 + \mathrm{i}p\sqrt{c_{55}/c_{22}}}, \quad C_{12} + C_{55} = \frac{c_{12} + c_{55}}{1 + \mathrm{i}p\sqrt{c_{55}/(c_{12} + c_{55})}},$$
$$C_{44} = \frac{C_{22} - C_{23}}{2} = \frac{c_{44}}{1 + \mathrm{i}p\sqrt{c_{55}C_{44}}}, \quad C_{55} = \frac{c_{55}}{1 + \mathrm{i}p} \tag{2a}$$

where $c_{ij}$ is the real, perfectly elastic stiffness constant and $p$ is the damping factor which can be expressed in the form,

$$p = p_0\left[1 + a_0\left(\frac{\omega}{\omega_0} - 1\right)^2 H\left(\frac{\omega}{\omega_0} - 1\right)\right] \tag{2b}$$

The parameter $p_0$ represents the effect of material dissipation, $a_0$ models the effect of scattering due to the fibers and other inhomogeneities, and $\omega_0$ is a frequency below which the scattering effect is negligible.

For multilayered laminates, each layer is assumed to be transversely isotropic, with its own axis of symmetry along the fibers, and is bonded to its neighbors with a thin layer of the matrix material. In the present analysis these interfacial layers are ignored for the sake of simplicity, but if needed, they can be incorporated in the analysis without difficulty.

## 3. The global matrix method for multilayered laminates

Elastodynamic analysis of multilayered composite laminates is difficult due to the complex behavior of the waves caused by their multiple reflection and transmission at the interlaminar interfaces and the boundaries of the laminate. This is due to the fact that, each incident ray at an interface produces three reflected waves and three transmitted rays, as shown in Mal et al. (1992b), in addition to diffracted waves and head waves. At the frequencies of interest here, the wavelengths are larger than the individual laminae, but can be smaller than the laminate thickness. Thus, the ray theoretical approach cannot be used to calculate the wavefield accurately. A wave theoretical treatment using multiple integral transforms and a matrix treatment proposed by the author has been found to be very effective in generating accurate numerical solutions to this class of problems. The details of the method can be found in a number of earlier papers (e.g., Mal and Lih, 1992; Lih and Mal, 1992, 1995, 1996; Mal, 1988), and will not be repeated here.

Three problems involving different types of sources that can be solved by this method are sketched in Fig. 1. The first problem, shown in Fig. 1a, models the so-called leaky Lamb wave (LLW) experiment in which the laminate is immersed in water and insonified by a beam of acoustic waves. The second problem, shown in Fig. 1b, is the dynamic surface source problem typical of low-frequency impact loading or high frequency ultrasonic testing. In the third problem, shown in Fig. 1c, the source of the waves is the sudden occurrence or extension of a delamination at an interface. In all three cases, the interest is the determination of the elastodynamic field in the laminate, and in the first problem, the acoustic field in the fluid as well. All

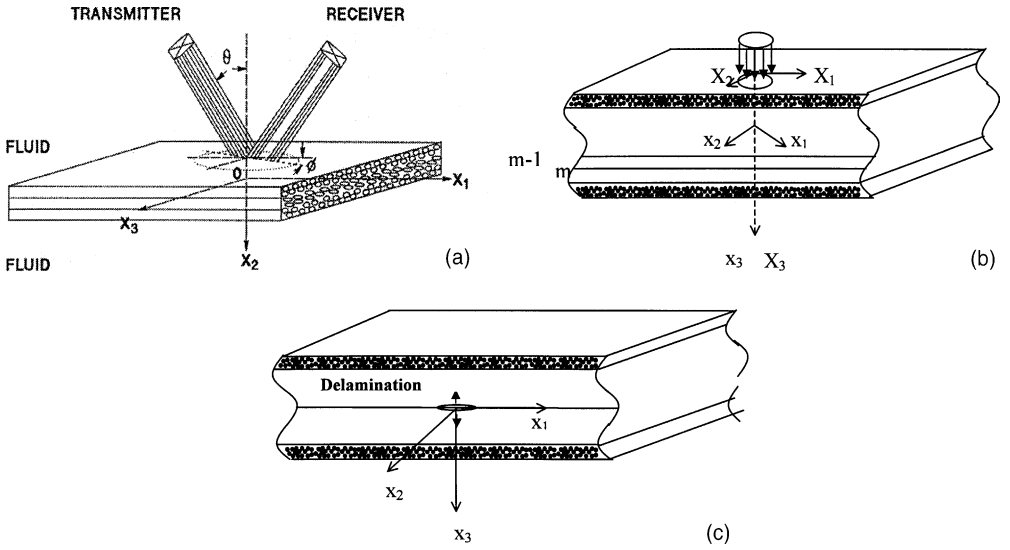


Fig. 1. Geometry of the composite laminate with three types of loading: (a) Acoustic wave loading in the leaky Lamb wave experiment. (b) Surface loading in foreign object impact. (c) Microfracture initiation at a damage site.

three problems can be formulated under the same general framework; they differ only in the specific forms of the boundary conditions.

In the problem shown in Fig. 1a, the boundary conditions at the top and bottom surfaces of the plate can be expressed in the form

$$\begin{aligned}\{\bar{S}(0)\} &= \{\,\bar{u}_0 \quad \bar{v}_0 \quad \mathrm{i}\eta_0(1-R) \quad 0 \quad 0 \quad -\rho\omega^2(1+R)\,\}\\ \{\bar{S}(H)\} &= \{\,\bar{u}_H \quad \bar{v}_H \quad \mathrm{i}\eta_0 T \quad 0 \quad 0 \quad -\rho\omega^2 T\,\}\end{aligned} \tag{3}$$

where $\bar{u}_0$, $\bar{v}_0$ are the Fourier time transforms of the horizontal and vertical components of the displacement on the top surface of the laminate, $\bar{u}_H$, $\bar{v}_H$ are those at the bottom surface, $\eta_0$ is the vertical wavenumber of the acoustic waves, $R$ is the reflection coefficient of the acoustic waves above the plate and $T$ is the transmission coefficient below the plate. In Eq. (3), $\{\bar{S}(\cdots)\}$ denotes the so-called stress displacement vector defined by $\{\bar{S}(x_i,\omega)\} = \{\{\bar{u}_i\}\{\bar{\sigma}_{i3}\}\}$. The reflected and transmitted waves can be calculated in the frequency domain or in the time domain (see, e.g., Mal et al., 1992b).

Another quantity that can be calculated from the theory is the dispersion equation for guided waves that can be transmitted along the laminate in the form

$$G(\omega, v, c_{ij}^m, \rho^m, h^m) = 0 \tag{4}$$

where $v$ is the velocity of the guided waves at frequency $\omega$. Eq. (4) is a nonlinear relation between the velocity of the multimode guided waves and the material properties of the laminate. For given laminate properties the dispersion curves can be determined from the equation. The dispersion curves can also be determined accurately from the LLW experiment, and for unidirectional composites the experimental dispersion data can be inverted to provide accurate estimates of the matrix dominated properties of the composite.

If there is an onset of delamination in a small area $A$ at the $p$th interface, as shown in Fig. 1c, then

$$[\overline{u}_i(X_1, X_2, X_3^p, \omega)]_-^+ = \overline{D}_i(\omega), \quad (X_1, X_2) \in A \tag{5}$$

where $[\ ]_-^+$ implies jump discontinuity across $A$, and $\bar{D}_i(\omega)$ is the Fourier time transform of the discontinuity. For assumed forms of the discontinuity, the wavefield produced in the laminate by the initiation or propagation of internal delaminations can be calculated (Guo et al., 1996). Accurate measurement of the wave signals by means of surface mounted transducers can be used to locate and characterize damage initiation and propagation in aircraft and other structures under service loads.

## 4. Approximate theory for thin laminates

If the thickness of the laminate, $H$, is much smaller than the wavelengths, then the problem can be solved by approximate methods. It is well known that the classical bending theory of the plate underestimates the deflections as well as the stresses and overestimates the phase velocity of the propagating waves. The classical theory becomes more and more inaccurate at higher frequencies. Refined higher order theories have been developed by many authors in an effort to improve the accuracy of the approximate results (Lih and Mal, 1995). The first order shear deformation plate theory (SDPT) retaining transverse shear and rotary inertia of the plate elements is used here. Assuming that the $xy$-plane is the mid-plane of the laminate, the displacement components within the laminate are assumed to be of the form

$$\begin{aligned} u(x,y,z,t) &= u_0(x,y,t) + z\psi_x(x,y,t) \\ v(x,y,z,t) &= v_0(x,y,t) + z\psi_y(x,y,t) \\ w(x,y,z,t) &= w_0(x,y,t) \end{aligned} \tag{6}$$

where ($u_0$, $v_0$, $w_0$) are the displacement components at a point in the mid-plane, and $\psi_x$ and $\psi_y$ are the rotations of a line element, originally perpendicular to the longitudinal plane, about the y and x axes, respectively. The solution of the resulting approximate system of equations can be obtained using multiple integral transforms (see, e.g., Lih and Mal, 1995; Guo et al., 1996).

## 5. Numerical results

### 5.1. Materials characterization using the leaky Lamb wave experiment

A major objective of the LLW experiment, shown in Fig. 1a, is to determine the elastic constants of the bulk composite material. The dispersion curves measured by this experiment can be inverted to yield accurate estimates of the matrix dominated elastic constants, $c_{22}$, $c_{23}$ and $c_{55}$ of the bulk composite material. The details of the experiment and the data inversion procedure can be found in Bar-Cohen et al. (1993). The theoretical and experimental dispersion curves for Lamb waves for a unidirectional composite plate are shown in Fig. 2. The dissipative properties of the material have negligible influence on the dispersion curves in the frequency range considered and were ignored in the theoretical model. The real elastic constants, determined through inversion of the LLW data using Eq. (4), are: $c_{11} = 161.31$ GPa, $c_{12} = 6.10$ GPa, $c_{22} = 13.90$ GPa, $c_{23} = 6.53$ GPa, $c_{55} = 7.26$ GPa. These values are substantially different from those calculated from homogenization theories using the constituent properties of graphite and epoxy.

It should be noted that the dispersion curves in the frequency range used in the experiment are not very sensitive to the elastic constants, $c_{11}$, $c_{12}$, and the dissipation constants, $p_0$, $a_0$ and $\omega_0$. Thus, the values of these parameters cannot be determined accurately from the measured dispersion curves. They require the use of time-of-flight or other data as discussed in Mal et al. (1992a) and Bar-Cohen et al. (1993). The waveforms recorded in a typical LLW experiment with incident angle 20° and three different fiber orientations on a 25 mm thick unidirectional graphite/epoxy laminate are shown in Fig. 3 together with

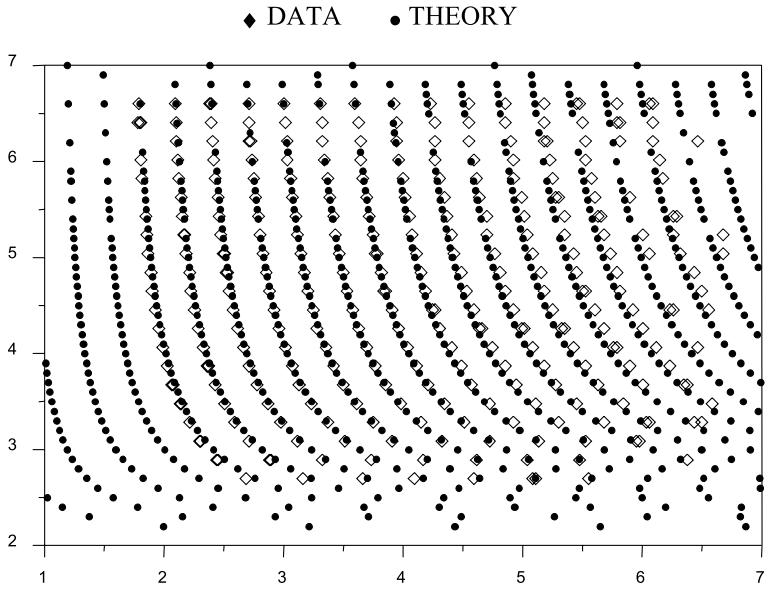


Fig. 2. Dispersion data for a defect-free 16-ply unidirectional Gr/Ep laminate of thickness 2.8 mm and density 1.59 g/cc.

calculated results using the exact theory. The elastic constants and the damping parameters that gave the best visual fit between the theoretical and experimental signals are given by:

$$\rho = 1.59\,\mathrm{g/cc}, \quad C_{11} = 160.7\ \mathrm{GPa}, \quad C_{12} = 6.4\ \mathrm{GPa}, \quad C_{22} = 13.9\ \mathrm{GPa}, \quad C_{23} = 6.9\ \mathrm{GPa},$$
$$C_{55} = 7.1\ \mathrm{GPa}, \quad p_0 = 0.01, \quad a_0 = 0.3, \quad \omega_0 = 0.6\pi.$$

### 5.2. Impact problems

The response of multilayered graphite/epoxy laminates with different ply configurations to a variety of dynamic surface loads has been calculated based on the exact and approximate theories described in Lih and Mal (1995) and Guo et al. (1996). The normal surface displacement produced in a 1 mm thick $[0, 90]_s$ cross-ply laminate by a concentrated unit (1 kN) normal force on its surface is shown in Fig. 4. The material properties of each lamina are assumed to be: $\rho = 1.58$ g/cc, $c_{11} = 160.7$ GPa, $c_{12} = 6.4$ GPa, $c_{22} = 13.9$ GPa, $c_{23} = 6.9$ GPa, $c_{55} = 7.1$ GPa, $p_0 = 0.005$, $a_0 = 0.1$, and $\omega_0 = 0.6\pi$. The time dependence of the force and its Fourier transform are given by

$$f(t) = \sin\frac{2\pi t}{\tau}, \quad 0 < t < \tau \tag{7}$$

$$\begin{aligned} F(\omega) &= \frac{\mathrm{i}\tau \sin(\omega\tau/2)}{\pi(1-\omega\tau/2\pi)}\mathrm{e}^{(-\mathrm{i}\omega\tau)/2}, \quad \omega \neq 2\pi/\tau \\ &= \frac{\mathrm{i}\pi}{\omega}\mathrm{e}^{(-\mathrm{i}\omega\tau)/2}, \quad \omega = 2\pi/\tau \end{aligned} \tag{8}$$

where $\tau$ is the duration of the source.

The calculated results using the exact theory and the approximate laminate theory are compared in Fig. 4 for different distances of propagation on a line oriented at 45° to the fibers. The duration of the source, $\tau$,

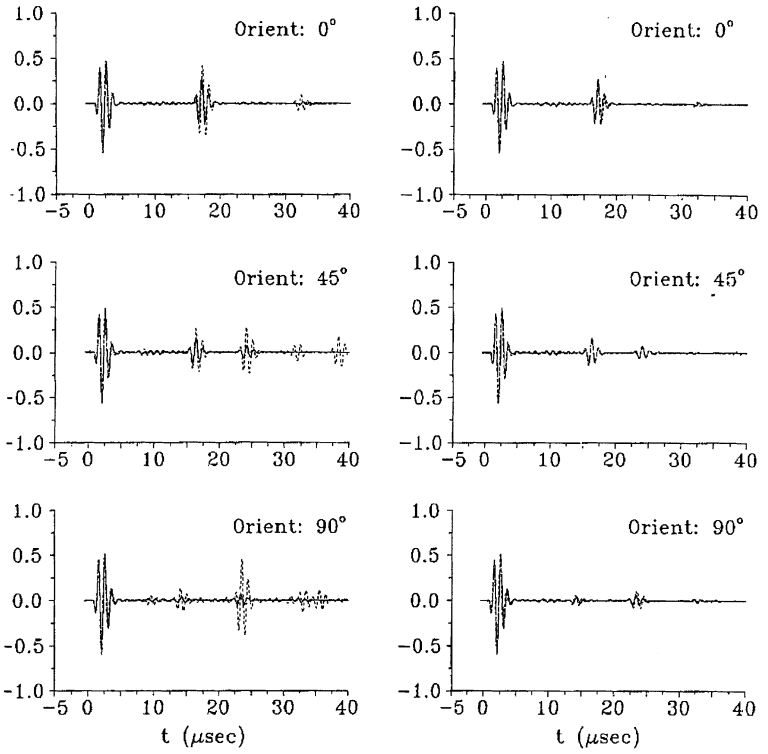


Fig. 3. Reflected acoustic waves from a 25 mm thick unidirectional graphite/epoxy plate recorded in the LLW experiment (solid curves) are compared with those calculated from the theoretical model (dashed curves) using perfectly elastic material in the left column and dissipative material in the right column.

is assumed to take on the values 5 and 0.5 μs in the two cases shown in Fig. 4a and b. It can be seen that for $\tau = 0.5$ μs (Fig. 4b), that the high frequency oscillations in the exact solution are absent in the approximate solution. The oscillations are caused by the reflection of the waves at the interfaces and these are smeared out in the laminate theory. The agreement between the exact and approximate results is improved significantly at $\tau = 5$ μs.

The main pulse in the time domain solution is caused by the plate guided flexural waves and these are reproduced well in the approximate solution, but their speed is overestimated, resulting in their earlier arrival at larger distances. Interface delamination is a common problem in composite structures when they are subjected to foreign object impact. Since delamination damage is often caused by the transverse stresses, $\sigma_{i3}$, at the interfaces, their determination is of great interest in developing strategies for predicting this critical damage in the structure. The theory described in Section 3 can be used to determine the transverse interfacial stresses in multilayered laminates subject to distributed surface loads. An example of this is given in Fig. 5, where the stress component, $\sigma_{33}$, at the topmost interface in a 1 mm thick $[0, 45, -45, 90]_s$ quasi-isotropic graphite/epoxy laminate produced by a distributed normal load in a circular area on its surface is calculated. The spatial dependence of the load is assumed to be a Gaussian and its time dependence is the same as in Eq. (7), i.e.,

$$f(x_1, x_2, t) = \mathrm{e}^{-(x_1^2+x_2^2)} \sin(2\pi t/\tau), \qquad (x_1^2 + x_2^2) < 1, \quad 0 < t < \tau \tag{9}$$

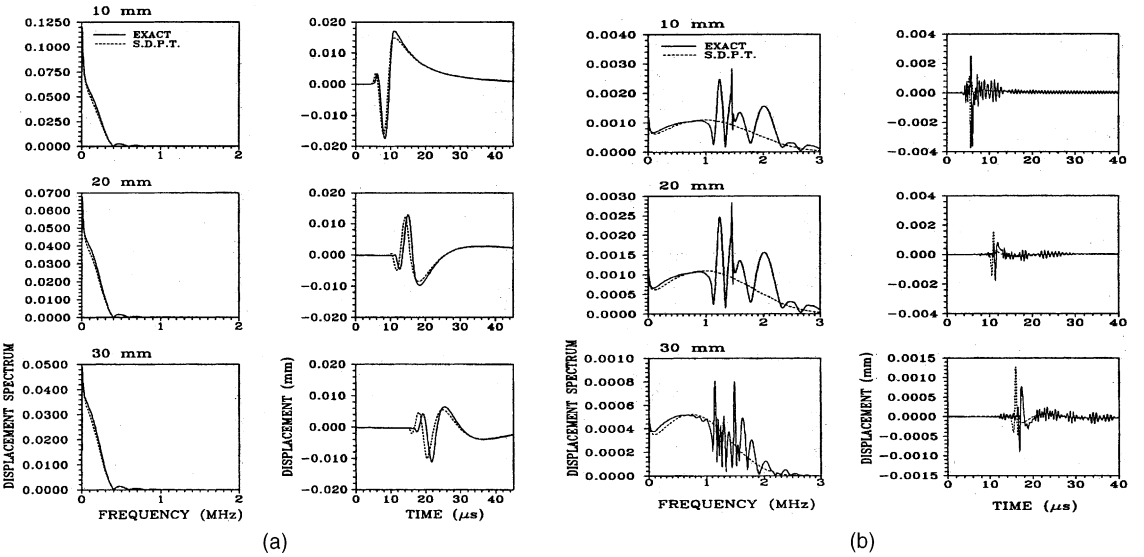


Fig. 4. Exact and approximate (SDPT) spectra and time histories of the normal surface displacement on a 1 mm thick $[0, 90]_s$ cross-ply laminate due to a unit concentrated force normal to the surface. The displacements are at points along a line through the source at 45° to the top fibers at different distance form the source, a single cycle of sine wave of duration 5 μs in (a) and 0.5 μs in (b).

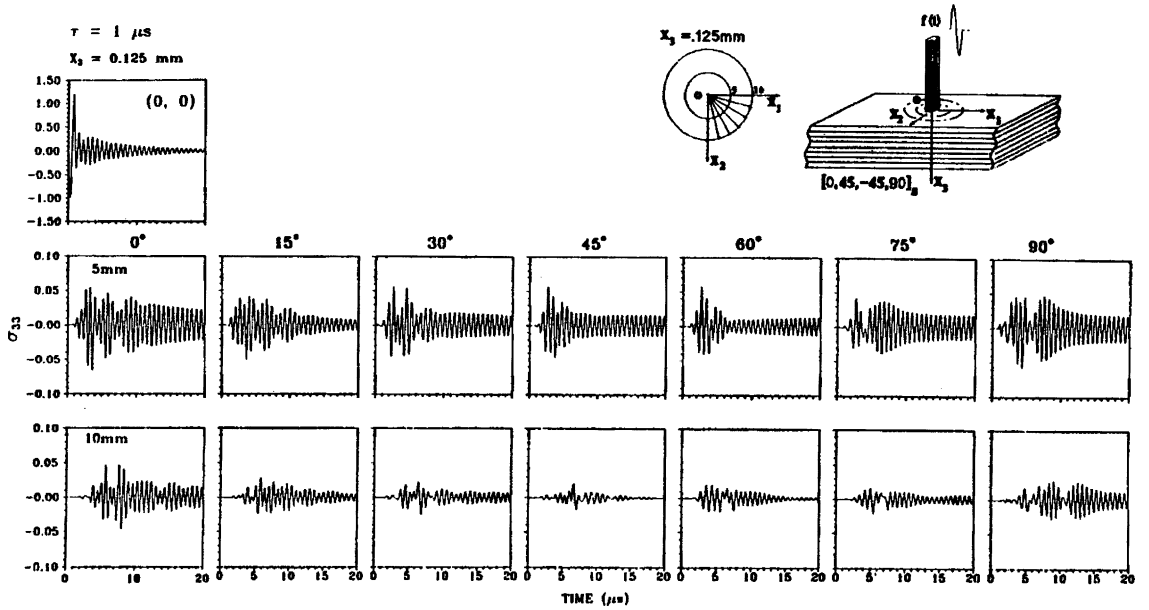


Fig. 5. Time histories of the stress component, $\sigma_{33}$ at the first interface in a 1 mm thick $[0, 45, -45, 90]_s$ laminate subject to a distributed normal surface force given in Eq. (9) on a circle of radius 1 mm. The angles indicate the polar angle of the field point relative to the fibers in the top lamina.

It can be seen that $\sigma_{33}$ has the general shape of the sign reversed force with superposed high frequency oscillations, that are less prominent for propagation near 45° to the fibers in the top lamina.

Low velocity impact tests on graphite epoxy panels of different configurations carried out recently by Shih and Mal (2000). The signals recorded from impact tests on a composite laminate were found to consist of two distinct signals: a relatively low frequency signal carried by the flexural waves produced at the onset of the impact load, followed by higher frequency signals generated from microfracture events occurring in the impact zone. There were also multiple reflections from the edges of the plate. Typical waveforms and frequency spectra of the flexural waves recorded in tests on a Gr/Ep laminate at different impact energies are shown in Fig. 6; they are in good agreement with calculations based on the theory described in Section 3 (not shown).

### 5.3. Radiation from initiation of microfracture

Composite materials are very sensitive to the presence of hidden flaws that may develop during their manufacturing, due to fatigue loading, and from foreign object impact during service. These defects, if undetected can grow to critical sizes, resulting in a serious degradation in the performance of composite structures and can compromise their safety. Thus, composite structures require careful monitoring of the initiation and growth of these flaws through nondestructive methods in order to insure their safety and integrity. At the present time periodic inspection and maintenance procedures are carried out on many aircraft and aerospace structures. These procedures are expensive and often unnecessary for a variety of reasons (see, e.g., Mal, 2000). Implementation of on-board continuous monitoring systems in defects critical structures can be very effective in dealing with this issue in aging as well as new structures. Recording and analysis of the elastic waves generated by crack initiation can be used to detect and characterize flaw initiation and growth in aircraft and aerospace structures. The basic idea behind such a system for a thin composite laminate used in aircraft components is described in this subsection.

A typical crack monitoring system is sketched in Fig. 7. It consists of a number of broadband sensors attached to the surface of the laminate. The waves generated by initiation of a new crack or the extension of an existing crack is simultaneously recorded by the sensors and stored in a computer. The theory developed in Section 3 can be used to locate the initiation site and to characterize some of the properties of the crack in the laminate. It can be shown that if the distance of the field point is more than twice the laminate thickness, then the motion at the field point is dominated by the plate-guided, multimode Lamb waves, and the surface displacement can be expressed as a sum of these modes (Guo et al., 1996). The number of modes depends on the dominant frequency of the source (i.e., its rise time) and the relative contributions from the modes depend on the detailed nature of the source including its location within the laminate.

In order to verify the accuracy of the approximate calculations, a pencil lead break source was used to generate and record the response on a unidirectional graphite epoxy plate of 1 mm thickness. The source can be represented by a vertical force, but its time dependence is not known a priori. The response of the measurement system is also unknown, as is the case with most such systems. The source time history modified by the system response was determined by measuring the surface Rayleigh wave response produced by the same source in a large aluminum block. The modified source time history is shown in Fig. 7(a). The normal displacement generated by the source was then calculated using the theory. The measured and calculated results are compared in Fig. 7 for three directions of propagation relative to the fibers. It can be seen that the agreement between the theoretical and experimental results are excellent in all three cases.

The radiation from the three major types of microfracture in thin multilayered composite laminates is considered next. A number of $[0, 90]_s$ cross-ply graphite/epoxy laminate coupon specimens of thickness 0.125 mm and lateral dimensions $100 \times 150$ mm with embedded defects were prepared in an autoclave, and subjected to fatigue loading in a servohydraulic test frame [INSTRON 8501]. The waves generated by crack initiation due to fiber break, matrix cracking and delamination, the three most common types of damage in

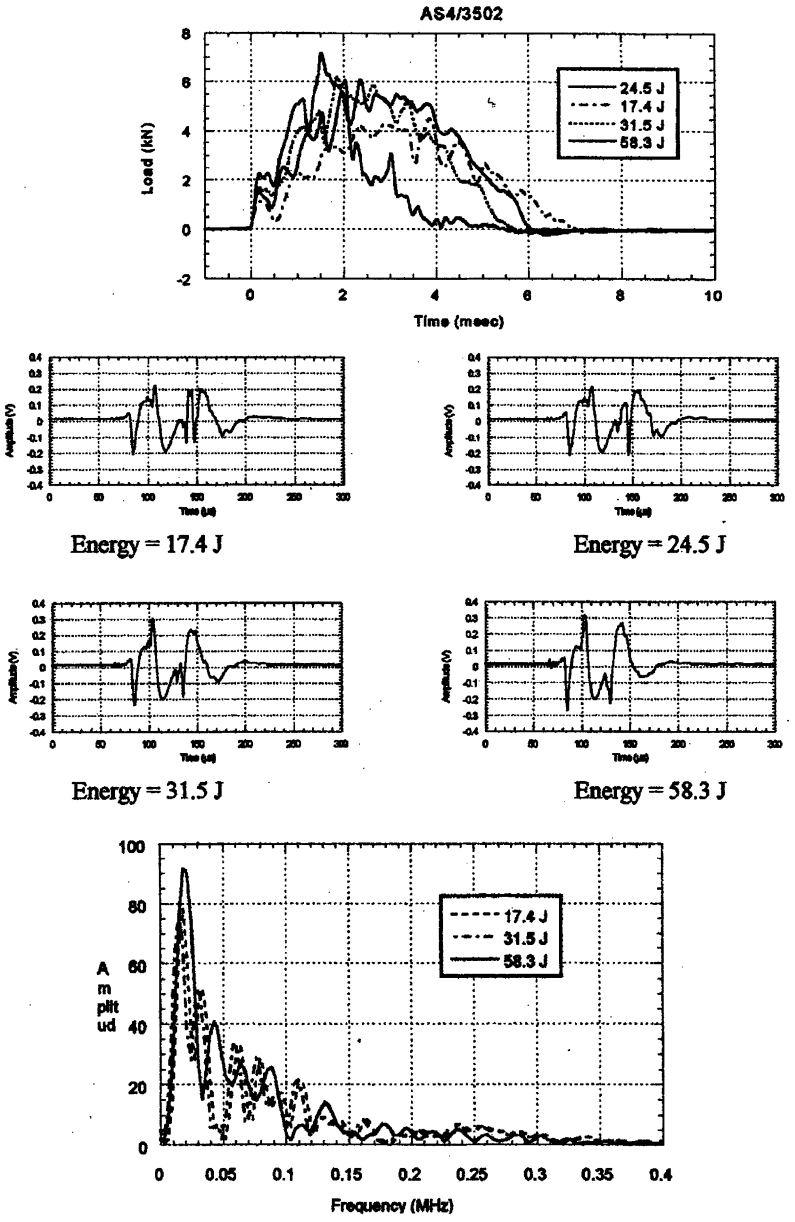


Fig. 6. Recorded contact force-time history, flexural waveforms and their spectra in low velocity impact tests on a cross-ply AS4/3502 laminate.

composite materials, were recorded by four broadband sensors attached to the sample during the tests. The details of the sample preparation and testing procedure can be found in Guo et al. (1996). Theoretical calculations of the Lamb waves from the sources were carried out using the laminate theory outlined in Section 4. The source time function was assumed to be of the form

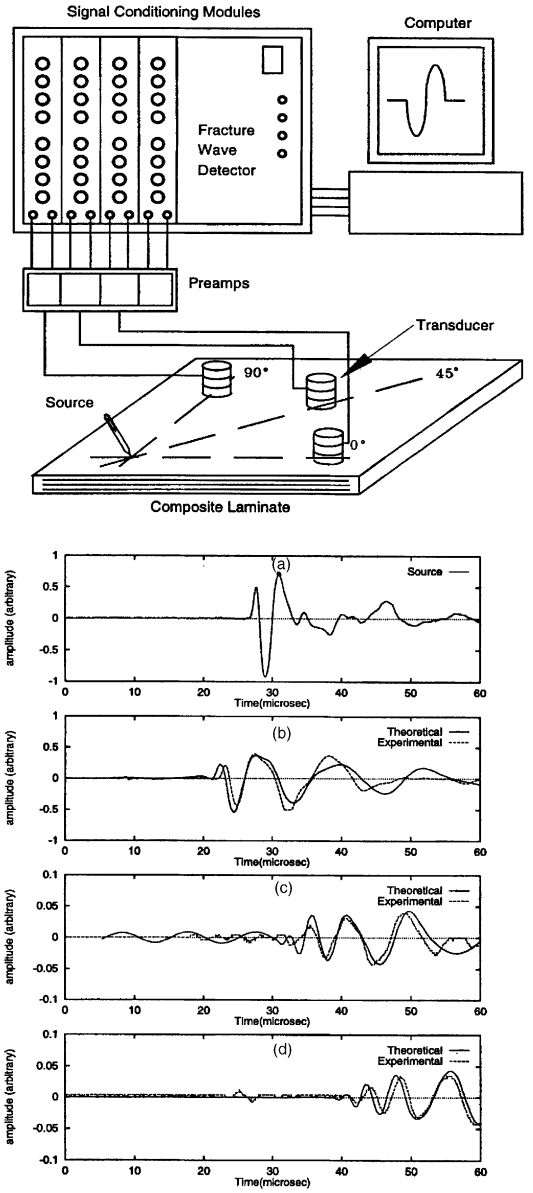


Fig. 7. Top: the ultrasonic experimental setup. Bottom: (a) modified source function for the pencil lead break including the response of the recording system, the surface response at (b) 0°, (c) 45°, and (d) 90° to the fibers in a 1 mm thick unidirectional graphite/epoxy plate. Calculated results are based on the approximate thin plate theory.

$$f(t) = \sin^2(\pi t/2\tau)H(t-\tau) \tag{10}$$

where $\tau$ is the rise time of the source and $H(t)$ is the Heaviside step function.

The experimental and theoretical results are compared in Fig. 8 for each type of damage initiation. The values of the rise time, $\tau$, that produced the best visual fit to the data were 0.5, 1.0 and 2 μs for fiber break,

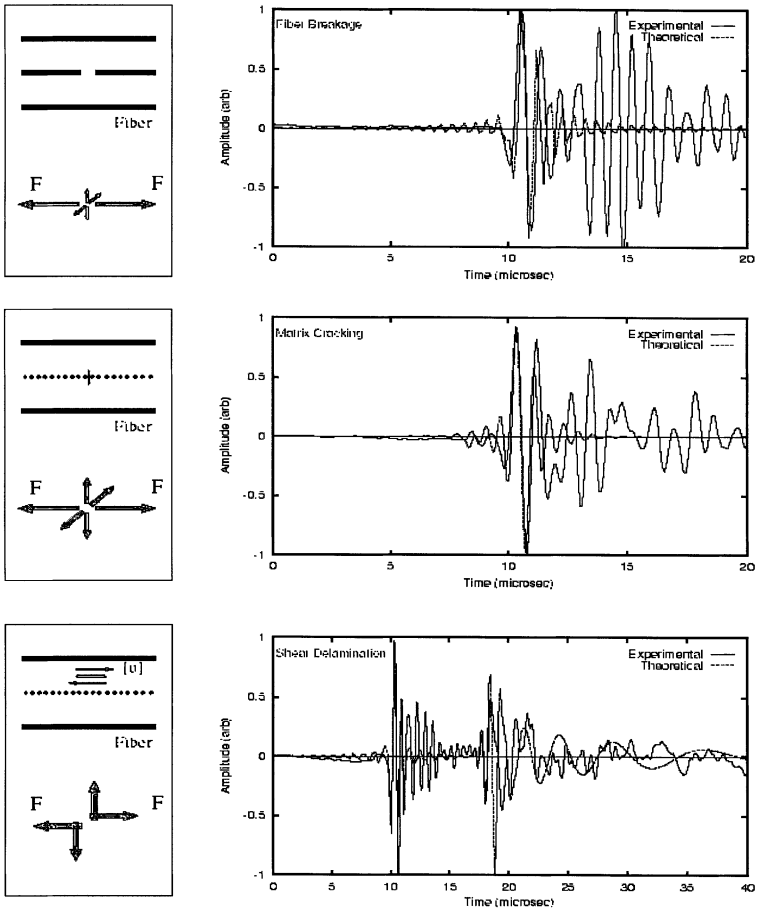


Fig. 8. Theoretical and experimental waveforms on the surface of a $[0, 90]_s$ cross-ply composite due to three types of microfracture sources. The calculations are based on thin plate theory.

matrix cracking and delamination, respectively. It should be noted that there is very good agreement between the calculated and measured displacements during the arrival of the main pulses from the source. The later arrivals in the experimental data are due to multiple reflections at the edges of the specimens and are not included in the theoretical model.

Another noteworthy feature of the results is the differences in the nature of the signals due to the three source types. The wave motion due to fiber break and matrix cracking are primarily the symmetric or extensional modes while that due to delamination contains both symmetric and antisymmetric (or flexural) modes (Guo et al., 1996). The difference in the properties of the signals generated by the three types of damage can be used to identify the onset or growth of delaminations during service in composite structures. The time histories and the spectral amplitude of the signals generated by the initiation of fiber break, matrix cracking and shear delamination in the middle layer of a $[0, 90]_s$ laminate are shown in Fig. 9. The differences in the properties of the signals are obvious—the first two types of damage generate mostly extensional waves of higher frequency, while the motion due to the delamination is dominated by flexural waves of lower frequency.

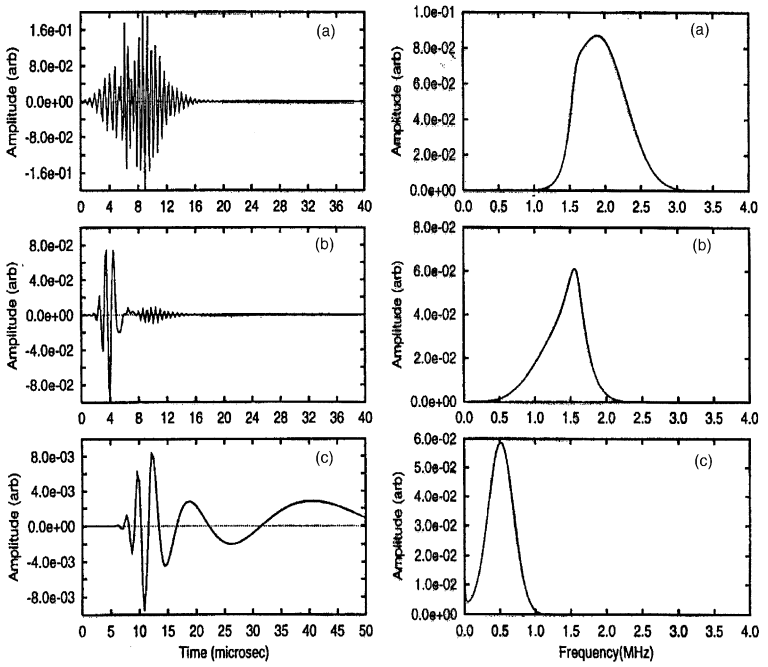


Fig. 9. Predicted differences in the signals and their spectra generated by (a) fiber break, (b) matrix cracking and (c) shear delamination, in a $[0, 90]_s$ cross-ply composite.

## 6. Concluding remarks

The elastic waves generated by three types of sources in composite laminates are investigated through laboratory experiments and theoretical models. The first source is a beam of acoustic waves incident on the laminate immersed in water, and is the basic feature in the so-called LLW experiment. The reflected acoustic waves were analyzed to determine the effective elastic constants and damping parameters of the material nondestructively. The second source is impact loading on the surface of the laminate, for which the surface displacement and interfacial stresses were calculated by means of exact and approximate theories. The accuracy of the approximate method was evaluated through comparison between the results obtained by the two methods. The third source is the initiation of three common types of damage, namely, fiber break, matrix cracking and delamination within the laminate. The signals produced by each type of damage were determined through laboratory experiments and theoretical modeling. The agreement between the two sets of results was found to be very good in all three cases. The differences in the signals generated by the three types of damage were evaluated. The results of this research can be very helpful in developing on-board health monitoring systems for aircraft, aerospace and other advanced structures (Mal, 2000; Haugse et al., 1999).

## References

Abrate, S., 1998. Impact on composite structures. Cambridge University Press, New York.

Bar-Cohen, Y., Mal, A.K., Lih, S.S., 1993. NDE of composite materials using ultrasonic oblique insonification. Materials Eval. 51, 1285–1296.

Guo, D., Mal, A.K., Ono, K., 1996. Wave theory of acoustic emission in composite laminates. J. Acoust. Emission 14, S19–S46.

Haugse, E., Leeks, T.J., Ikegami, R., Johnson, P.E., Ziola, S.M., Doroghi, J.F., May, S., Phelps, N., 1999. Crack growth detection and monitoring using broadband acoustic emission technique. In: Nondestructive Evaluation of Aging Aircraft, Airports, and Aerospace hardware III. In: Mal, A. (Ed.), Proceedings of SPIE Conference, 3586, pp. 32–40.

Lih, S.-S., Mal, A.K., 1992. Elastodynamic response of a unidirectional composite laminate to concentrated surface loads: Part II. J. Appl. Mech. 59, 887–892.

Lih, S.-S., Mal, A.K., 1995. On the accuracy of approximate plate theories for wave field calculations in composite laminates. Wave Motion 21, 17–34.

Lih, S.-S., Mal, A.K., 1996. Response of multilayered composite laminates to dynamic surface loads. Composites B 29B, 633–641.

Mal, A.K., 1988. Wave propagation in layered composite laminates under periodic surface loads. Wave Motion 10, 257–266.

Mal, A.K., 2000. The role of NDE in structural health monitoring of aircraft and aerospace structures. In: SPIE Conf. on NDE of Aging Aircraft, Airports and Aerospace Hardware, 3994. Newport Beach, California, pp. ix–xiii.

Mal, A.K., Lih, S.-S., 1992. Elastodynamic response of a unidirectional composite laminate to concentrated surface loads: Part I. J. Appl. Mech. 59, 878–886.

Mal, A.K., Singh, S., 1991. Deformation of elastic solids. Prentice Hall, New Jersey.

Mal, A.K., Bar-Cohen, Y., Lih, S.S., 1992a. Wave attenuation in fiber-reinforced composites. In: Proceedings of International Conference on Mechanics and Mechanisms of Material Damping, 1169. ASTM STP, pp. 245–261.

Mal, A.K., Yin, C.-C., Bar-Cohen, Y., 1992b. Analysis of acoustic pulses reflected from fiber-reinforced composites. J. Appl. Mech. 59, 136–144.

Shih, J.H., Mal, A.K., 2000. Acoustic Emission from Impact Damage in Cross-Ply Composites. In: Chang, F.-K. (Ed.), Structural Health Monitoring, 1, pp. 209–217.